

Studying the potential of QQq at finite temperature in a holographic model

Xun Chen(陈勋)^{1;1)} Bo Yu(喻博)¹ Peng-Cheng Chu(初鹏程)^{2,3;2)} Xiao-hua Li(李小华)^{1;3)}

¹ School of Nuclear Science and Technology, University of South China, Hengyang 421001, China

² The Research Center for Theoretical Physics, Science School, Qingdao University of Technology, Qingdao 266033, China

³ The Research Center of Theoretical Physics, Qingdao University of Technology, Qingdao 266033, China

Abstract: Using gauge/gravity duality, we investigate the string breaking and dissolution of two heavy quarks coupled to a light quark at finite temperature. It is found that three configurations of QQq exist with the increase in separation distance for heavy quarks in the confined phase. Furthermore, string breaking occurs at the distance $L_{\text{QQq}} = 1.27\text{fm}(T = 0.1\text{GeV})$ for the decay mode $\text{QQq} \rightarrow \text{Qq} + \text{Q}\bar{q}$. In the deconfined phase, QQq melts at a certain distance then becomes free quarks. Finally, we compare the potential of QQq with that of $\text{Q}\bar{\text{Q}}$ and it is found that $\text{Q}\bar{\text{Q}}$ is more stable than QQq at high temperature.

Key words: doubly heavy baryons, holographic QCD, potential

1 Introduction

With over 20 years of development, gauge/gravity duality has become a useful tool to deal with the QCD problem through gravitational theory. Quark-antiquark potential is one of the hottest topics in holographic QCD, because heavy quarkonia are among the most sensitive probes used in the experimental study of quark-gluon plasma (QGP) and its properties. The holographic potential of the quark-antiquark pair was first recorded in Ref.[1]. It was found that the quark-antiquark potential exhibits a purely Coulombian (non-confining) behavior and agrees with a conformal gauge theory. Soon after, the potential at finite temperature was been discussed in [2, 3]. The deformed AdS_5 model and Einstein-Maxwell-Dilation models were used to calculate the quark-antiquark potential in these studies[4–27].

Moreover, the recent discovery of a doubly charmed baryon (DHB) $\Xi_{cc}+$ through LHCb experiments at CERN[28, 29] has reinforced interest in the search for a theoretical description of doubly heavy baryons. Inside a DHB, there is a heavy diquark and light quark. Because the heavy quark in a DHB is almost near its mass shell, it is reasonable to expect the heavy quark limit to be applicable in this system[30]. Although lattice gauge theory remains a basic tool for studying nonperturbative phenomena in QCD, it has achieved limited results on QQq potentials to date [31, 32].

In recent years, the multi-quark potential from the holographic model has been discussed by Oleg Andreev in Ref.[33–37]. In this effective string model, heavy quarks are connected by string to a baryon vertex whose

action is given by a five brane wrapped around an internal space, and the light quark is a tachyon field coupled to the worldsheet boundary. The main reason for pursuing this model is that its results on the quark-antiquark and three-quark potentials are consistent with lattice calculations and QCD phenomenology[4, 33–37]. The technology we use to extract the QQq potential is same as at in lattice QCD[38]. The QQq potential is extracted from the expectation value of the QQq Wilson loop $W_{\text{QQq}}(R, T)$. The QQq Wilson loop is constructed from the heavy-quark trajectories and light-quark propagator. Hence, we investigate the QQq potential at finite temperature in this paper using gauge/gravity duality.

The remainder of this paper is organized as follows: We establish the different configurations of string at finite temperature in Sec.2. Then, we numerically solve these configurations at different temperatures and provide a discussion in Sec.3. In Sec.4, we discuss string breaking for the confined phase. Finally, the summary and conclusion are given in Sec.5.

2 Connected string configuration

First, we briefly review the holographic model used in the paper. Following Ref. [35], this background metric at finite temperature is

$$ds^2 = e^{sr^2} \frac{R^2}{r^2} (f(r)dt^2 + d\vec{x}^2 + f^{-1}(r)dr^2) + e^{-sr^2} g_{ab}^{(5)} d\omega^a d\omega^b. \quad (1)$$

This model parameterized by s is a one-parameter deformation of Euclidean AdS_5 space with a constant radius R , and a five-dimensional compact space (sphere)

1) E-mail: chenxunhep@qq.com

2) E-mail: kyois@126.com

3) E-mail: lixiaohuaphysics@126.com

\mathbf{X} , whose coordinates are ω^a and $f(r)$, is a blackening factor. The Nambu-Goto action of a string is expressed as

$$S = \frac{1}{2\pi\alpha'} \int_0^1 d\sigma \int_0^T d\tau \sqrt{\gamma}, \quad (2)$$

where γ is an induced metric on the string world-sheet (with a Euclidean signature). For AdS_5 space, $f(r) = 1 - \frac{r^4}{r_h^4}$ with the boundary conditions $f(0) = 1$ and $f(r_h) = 0$. r_h is the position of the black hole(brane). The Hawking temperature identified with the temperature of a dual gauge theory can be defined as $T = \frac{1}{4\pi} |\partial_r f|_{r=r_h}$. The motivations for this metric have been clarified in Ref. [35]. However, such a deformed AdS_5 metric leads to linear Regge-like spectra for mesons[39, 40] and the Cornell potential of a quark-antiquark [4]. The deformed metric satisfies the thermodynamics of lattice[41].

Subsequently, we introduce the baryon vertex. According to the AdS/CFT correspondence, this is a five brane[42]. At leading order in α' , the brane action is $S_{vert} = \mathcal{T}_5 \int d^6\xi \sqrt{\gamma^{(6)}}$, where \mathcal{T}_5 is the brane tension, and ξ^i are the world-volume coordinates. Because the brane is wrapped around the internal space, it appears point-like in AdS_5 . We choose a static gauge $\xi^0 = t$ and $\xi^a = \theta^a$ with θ^a coordinates on \mathbf{X} . Thus, the action is

$$S_{vert} = \tau_v \int dt \frac{e^{-2sr^2}}{r} \sqrt{f(r)}, \quad (3)$$

where τ_v is a dimensionless parameter defined by $\tau_v = \mathcal{T}_5 R \text{vol}(\mathbf{X})$ and $\text{vol}(\mathbf{X})$ is a volume of \mathbf{X} .

Finally, we consider that the light quark at string endpoints is a tachyon field, which couples to the world-sheet boundary via $S_q = \int d\tau e \mathbf{T}$; this is the usual sigma-model action for a string propagating in the tachyon background[43]. The integral is over a world-sheet boundary parameterized by τ , and e is a boundary metric. We consider a constant background $\mathbf{T}(x, r) = \mathbf{T}_0$ and worldsheets whose boundaries are lines in the t direction. Thus, the action can be written as

$$S_q = m \int dt \frac{e^{\frac{5}{2}r^2}}{r} \sqrt{f(r)}, \quad (4)$$

where $m = R \mathbf{T}_0$. This is the action of a point particle of mass \mathbf{T}_0 at rest. We choose the model parameters as follows: $\mathbf{g} = \frac{R^2}{2\pi\alpha'}$, $\mathbf{k} = \frac{\tau_v}{3\mathbf{g}}$, and $\mathbf{n} = \frac{m}{\mathbf{g}}$.

2.1 Small L

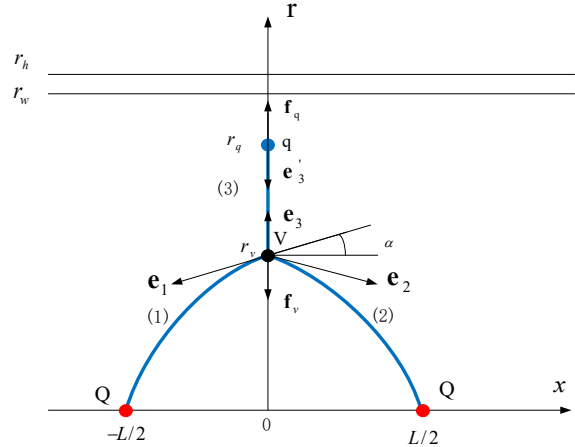


Fig. 1. Static string configuration at a small separation distance of a heavy-quark pair. The heavy quarks Q are placed on the x -axis, while the light quark q and baryon vertex V are on the r -axis, at $r = r_q$ and $r = r_v$ respectively. The quarks and baryon vertex are connected by the blue string. The force exerted on the vertex and light quark are depicted by the black arrows. r_h is the position of the black-hole horizon. r_w is the position of a soft wall in the confined phase.

The configuration of QQq is plotted in Fig.1. The total action is the sum of the Nambu-Goto actions plus the actions for the vertex and background scalar.

$$S = \sum_{i=1}^3 S_{NG}^{(i)} + S_{vert} + S_q. \quad (5)$$

If we choose the static gauge $\xi^1 = t$ and $\xi^2 = r$, the boundary conditions for $x(r)$ become

$$x^{(1)}(0) = -\frac{L}{2}, \quad x^{(2)}(0) = \frac{L}{2}, \quad x^{(i)}(r_v) = x^{(3)}(r_q) = 0. \quad (6)$$

The action can now be written as

$$S = \mathbf{g}T \left(2 \int_0^{r_v} \frac{dr}{r^2} e^{sr^2} \sqrt{1 + f(r)} (\partial_r x)^2 + \int_{r_v}^{r_q} \frac{dr}{r^2} e^{sr^2} \sqrt{1 + f(r)} (\partial_r x)^2 + 3\mathbf{k} \frac{e^{-2sr_v^2}}{r_v} \sqrt{f(r_v)} + \mathbf{n} \frac{e^{\frac{5}{2}sr_q^2}}{r_q} \sqrt{f(r_q)} \right), \quad (7)$$

where $\partial_r x = \frac{\partial x}{\partial r}$ and $T = \int_0^T dt$. We consider the first term in (7), which corresponds to string (1) and (2) in Fig. 1. The equation of motion(EoM) for $x(r)$ can be obtained from the Euler-Lagrange equation. Thus, we have

$$\mathcal{I} = \frac{w(r)f(r)\partial_r x}{\sqrt{1+f(r)(\partial_r x)^2}}, \quad w(r) = \frac{e^{sr^2}}{r^2}. \quad (8)$$

\mathcal{I} is a constant. At r_v , we have $\partial_r x|_{r=r_v} = \cot \alpha$ with $\alpha > 0$ and

$$\mathcal{I} = \frac{w(r_v)f(r_v)\cot \alpha}{\sqrt{1+f(r_v)(\cot \alpha)^2}}. \quad (9)$$

$\partial_r x$ can be solved as

$$\partial_r x = \sqrt{\frac{\omega(r_v)^2 f(r_v)^2}{(f(r_v) + \tan^2 \alpha) \omega(r)^2 f(r)^2 - f(r) w(r_v)^2 f(r_v)^2}}. \quad (10)$$

Using (10), the integral over $[0, r_v]$ of dr is

$$L = 2 \int_0^{r_v} \frac{dr}{\partial_r x}. \quad (11)$$

L is a function of r_v , α , and r_h (or equally, temperature). The energy of string (1) can be found from the first term of (7):

$$E_R = \frac{S}{T} = \mathbf{g} \int_0^{r_v} \frac{dr}{r^2} e^{sr^2} \sqrt{1+f(r)(\partial_r x)^2}. \quad (12)$$

Subtracting the divergent term $\mathbf{g} \int_0^\infty dr \frac{1}{r^2}$, we have the regularized energy:

$$E_1 = \frac{S}{T} = \mathbf{g} \int_0^{r_v} \left(\frac{1}{r^2} e^{sr^2} \sqrt{1+f(r)(\partial_r x)^2} - \frac{1}{r^2} \right) dr - \frac{\mathbf{g}}{r_v} + c. \quad (13)$$

Here c is a normalization constant. because string (2) produces the same results, we move to string (3) whose action is given by the second term in (7). This string is a straight string stretched between the vertex and light. The energy can be calculated as

$$E_2 = \mathbf{g} \int_{r_v}^{r_q} \frac{dr}{r^2} e^{sr^2}. \quad (14)$$

Now, we can present the energy of the configuration. From (7), it follows that

$$\begin{aligned} E_{QQ_q} = & \mathbf{g} \left(2 \int_0^{r_v} \left(\frac{1}{r^2} e^{sr^2} \sqrt{1+f(r)(\partial_r x)^2} - \frac{1}{r^2} \right) dr - \frac{2}{r_v} \right. \\ & + \int_{r_v}^{r_q} \frac{dr}{r^2} e^{sr^2} + n \frac{e^{\frac{1}{2}sr_q^2}}{r_q} \sqrt{f(r_q)} + 3k \frac{e^{-2sr_v^2}}{r_v} \sqrt{f(r_q)} \\ & \left. + 2c. \right) \quad (15) \end{aligned}$$

The energy is also a function of r_v , α , and r_h . There are two steps to be completed: The first is to determine the position of the light quark, which is a function of temperature, and the second is to determine α . To achieve

this goal, the net forces exerted on the light quark and vertex vanish. We first write the force balance equation of the light quark as

$$\mathbf{f}_q + \mathbf{e}'_3 = 0. \quad (16)$$

By varying the action with respect to r_q , it is found that $\mathbf{f}_q = \left(0, -\mathbf{g}n\partial_{r_q} \left(\frac{e^{\frac{1}{2}sr_q^2}}{r_q} \sqrt{f(r_q)} \right) \right)$ and $\mathbf{e}'_3 = \mathbf{g}w(r_q)(0, -1)$. Hence, the force balance equation becomes

$$2e^{\frac{r_q^2 s}{2}} \sqrt{f(r_q)} + 2n(-1+r_q^2 s) f(r_q) + nr_q f'(r_q) = 0. \quad (17)$$

Note that r_q (the position of the light quark) is only a function of r_h . At fixed temperature, r_q can be fixed via the above equation. The force balance equation on the vertex is

$$\mathbf{e}_1 + \mathbf{e}_2 + \mathbf{e}_3 + \mathbf{f}_v = 0. \quad (18)$$

Here \mathbf{e}_i is the string tension which can be calculated in the same manner as in Ref.[37]. As a result, the force on the vertex is $\mathbf{f}_v = \left(0, -3\mathbf{g}k\partial_{r_v} \left(\frac{e^{-2sr_v^2}}{r_v} \sqrt{f(r_v)} \right) \right)$, and the string tensions are $\mathbf{e}_1 = \mathbf{g}w(r_v) \left(-\frac{f(r_v)}{\sqrt{\tan^2 \alpha + f(r_v)}}, -\frac{1}{\sqrt{f(r_v)\cot^2 \alpha + 1}} \right)$, $\mathbf{e}_2 = \mathbf{g}w(r_v) \left(\frac{f(r_v)}{\sqrt{\tan^2 \alpha + f(r_v)}}, -\frac{1}{\sqrt{f(r_v)\cot^2 \alpha + 1}} \right)$, $\mathbf{e}_3 = \mathbf{g}w(r_v)(0, 1)$. The non-trivial component of the force balance equation is

$$2e^{3sr_v^2} \left(1 - \frac{2}{1 + \cot^2 \alpha f(r_v)} \right) + 6(k + 4ksr_v^2) \sqrt{f(r_v)} - \frac{3kr_v f'(r_v)}{\sqrt{f(r_v)}} = 0. \quad (19)$$

This equation provides the relationship between r_v and α when the temperature is fixed. With (15) and (17), we can numerically solve the energy at small L .

2.2 Intermediate L

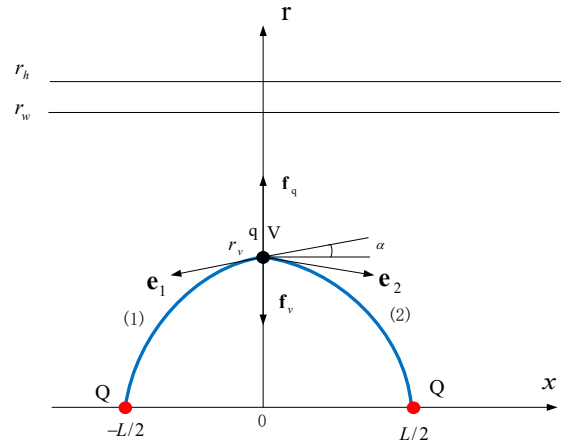


Fig. 2. Static string configuration at an intermediate separation distance of a heavy-quark pair. The heavy quarks Q are placed on the x-axis, while the light quark q and baryon vertex V are at the same point r_v on the r-axis. The forces exerted on the point are depicted by the black arrows. r_h is the position of the black-hole horizon. r_w is the position of a soft wall in the confined phase.

The total action of the configuration plotted in Fig.2 is expressed as

$$S = \sum_{i=1}^2 S_{\text{NG}}^{(i)} + S_{\text{vert}} + S_q. \quad (20)$$

We still choose the same static gauge as before. The boundary conditions then take the form

$$x^{(1)}(0) = -\frac{L}{2}, \quad x^{(2)}(0) = \frac{L}{2}, \quad x^{(i)}(r_v) = 0. \quad (21)$$

In this configuration, the expressions (11) and (13) still hold. Naturally, we can express the total energy of the string without the contribution from string (3) as follows:

$$E_{QQq} = \mathbf{g} \left(2 \int_0^{r_v} \left(\frac{1}{r^2} e^{sr^2} \sqrt{1 + f(r)} (\partial_r x)^2 - \frac{1}{r^2} \right) dr - \frac{2}{r_v} \right. \\ \left. + n \frac{e^{\frac{1}{2} sr_v^2}}{r_v} \sqrt{f(r_v)} + 3k \frac{e^{-2sr_v^2}}{r_v} \sqrt{f(r_v)} \right) + 2c. \quad (22)$$

The force balance equation at the point $r = r_v$ is

$$\mathbf{e}_1 + \mathbf{e}_2 + \mathbf{f}_v + \mathbf{f}_q = 0. \quad (23)$$

Each force is given by

$$\mathbf{f}_q = \left(0, -n \mathbf{g} k \partial_{r_q} \left(\frac{e^{\frac{1}{2} sr_q^2}}{r_q} \sqrt{f(r_q)} \right) \right),$$

$$\mathbf{f}_v = \left(0, -3 \mathbf{g} k \partial_{r_v} \left(\frac{e^{-2sr_v^2}}{r_v} \sqrt{f(r_v)} \right) \right),$$

$$\mathbf{e}_1 = \mathbf{g} w(r_v) \left(-\frac{f(r_v)}{\sqrt{\tan^2 \alpha + f(r_v)}}, -\frac{1}{\sqrt{f(r_v) \cot^2 \alpha + 1}} \right),$$

$$\mathbf{e}_2 = \mathbf{g} w(r_v) \left(\frac{f(r_v)}{\sqrt{\tan^2 \alpha + f(r_v)}}, -\frac{1}{\sqrt{f(r_v) \cot^2 \alpha + 1}} \right),$$

where $r_q = r_v$. The force balance equation leads to

$$2 \left(-e^{\frac{5r_v^2 s}{2}} n (-1 + r_v^2 s) + 3k (1 + 4r_v^2 s) \right) \sqrt{f(r_v)} \\ - \frac{4e^{3r_v^2 s}}{\sqrt{1 + \cot^2 \alpha} f(r_v)} - \frac{(3k + e^{\frac{5r_v^2 s}{2}}) r_v f'(r_v)}{\sqrt{f(r_v)}} = 0. \quad (24)$$

2.3 Large L

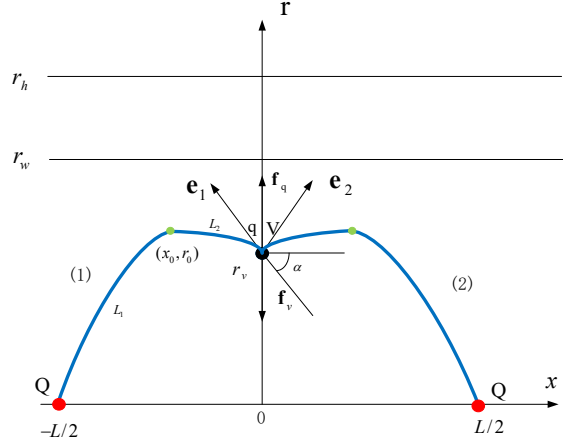


Fig. 3. Static string configuration at A large separation distance of a heavy-quark pair. The heavy quarks Q are placed on the x-axis, while the light quark q and baryon vertex V are at the same point r_v on the r-axis. The forces exerted on the point are depicted by the black arrows. There is a turning point located at (x_0, r_0) for string (1). r_w is the position of a soft wall in the confined phase. r_h is the position of the black-hole horizon.

The total action of the configuration plotted in Fig.3 is the same as Eq. (20). However, it is convenient to choose another static gauge $\xi^1 = t$ and $\xi^2 = x$ here. Then, the boundary conditions are

$$r^{(1)}(-L/2) = r^{(2)}(L/2) = 0, \quad r^{(i)}(0) = r_v. \quad (25)$$

The total action becomes

$$S = \mathbf{g} T \left(\int_{-L/2}^0 dx w(r) \sqrt{f(r) + (\partial_x r)^2} + \int_0^{L/2} dx w(r) \sqrt{f(r) + (\partial_x r)^2} \right. \\ \left. + 3k \frac{e^{-2sr_v^2}}{r_v} \sqrt{f(r_v)} + n \frac{e^{\frac{1}{2} sr_v^2}}{r_v} \sqrt{f(r_v)} \right). \quad (26)$$

We consider string (1), whose action is given by the first term in (26). The first integral has the form

$$\mathcal{I} = \frac{w(r) f(r)}{\sqrt{f(r) + (\partial_x r)^2}}. \quad (27)$$

At points r_0 and r_v , we have

$$\frac{w(r) f(r)}{\sqrt{f(r) + (\partial_x r)^2}} = w(r_0) \sqrt{f(r_0)}, \quad (28)$$

$$\frac{w(r) f(r)}{\sqrt{f(r) + \tan^2 \alpha}} = w(r_0) \sqrt{f(r_0)}. \quad (29)$$

The relationship between r_0 , r_v , and α can be obtained from Eq. (29). Using Eq. (28), the separation distance and energy can be subsequently obtained. As before, $\partial_x r$ can be solved as

$$\partial_x r = \sqrt{\frac{w(r)^2 f(r)^2 f(r_0) - f(r) w(r_0)^2 f(r_0)^2}{w(r_0)^2 f(r_0)^2}}. \quad (30)$$

The separation distance consists of two parts:

$$\begin{aligned} L &= 2(L_1 + L_2) = 2\left(\int_0^{r_0} \frac{1}{r'} dr + \int_{r_v}^{r_0} \frac{1}{r'} dr\right) \\ &= 2\left(\int_0^{r_0} \sqrt{\frac{w(r_0)^2 f(r_0)^2}{w(r)^2 f(r)^2 f(r_0) - f(r) w(r_0)^2 f(r_0)^2}} dr \right. \\ &\quad \left. + \int_{r_v}^{r_0} \sqrt{\frac{w(r_0)^2 f(r_0)^2}{w(r)^2 f(r)^2 f(r_0) - f(r) w(r_0)^2 f(r_0)^2}} dr\right). \end{aligned} \quad (31)$$

The energy of string (1) can be obtained by summing two parts:

$$\begin{aligned} E_R &= E_{R_1} + E_{R_2} \\ &= \mathbf{g} \int_0^{r_0} w(r) \sqrt{1 + f(r) x'^2} dr + \mathbf{g} \int_{r_v}^{r_0} w(r) \sqrt{1 + f(r) x'^2} dr \\ &= \mathbf{g} \int_0^{r_0} w(r) \sqrt{\frac{w(r)^2 f(r)^2 f(r_0)}{w(r)^2 f(r)^2 f(r_0) - f(r) w(r_0)^2 f(r_0)^2}} dr \\ &\quad + \mathbf{g} \int_{r_v}^{r_0} w(r) \sqrt{\frac{w(r)^2 f(r)^2 f(r_0)}{w(r)^2 f(r)^2 f(r_0) - f(r) w(r_0)^2 f(r_0)^2}} dr. \end{aligned} \quad (32)$$

After subtracting the divergent term, the renormalized energy of string (1) is

$$\begin{aligned} E &= \mathbf{g} \int_{r_v}^{r_0} (w(r) \sqrt{\frac{w(r)^2 f(r)^2 f(r_0)}{w(r)^2 f(r)^2 f(r_0) - f(r) w(r_0)^2 f(r_0)^2}}) dr \\ &\quad + \mathbf{g} \int_0^{r_0} (w(r) \sqrt{\frac{w(r)^2 f(r)^2 f(r_0)}{w(r)^2 f(r)^2 f(r_0) - f(r) w(r_0)^2 f(r_0)^2}} \\ &\quad - \frac{1}{r^2}) dr - \frac{1}{r_0} + 2c \end{aligned} \quad (33)$$

The calculation of string (2) has the same procedure as before and gives the same expressions for L and E . Then, the total energy of the configuration can be written as

$$\begin{aligned} E_{QQq} &= \left(2 \int_{r_v}^{r_0} w(r) \sqrt{\frac{w(r)^2 f(r)^2 f(r_0)}{w(r)^2 f(r)^2 f(r_0) - f(r) w(r_0)^2 f(r_0)^2}} \right. \\ &\quad \left. dr + 2 \int_0^{r_0} (w(r) \sqrt{\frac{w(r)^2 f(r)^2 f(r_0)}{w(r)^2 f(r)^2 f(r_0) - f(r) w(r_0)^2 f(r_0)^2}} \right. \\ &\quad \left. - \frac{1}{r^2}) dr - \frac{1}{r_0} + 3k \frac{e^{-2sr_v}}{r_v} + n \frac{e^{\frac{1}{2}sr_v^2}}{r_v} \right) \mathbf{g} + 2c. \end{aligned} \quad (34)$$

The force balance equation is the same as Eq. (23). Each force is similarly given in the previous section. With Eq. (29) and (24), we can numerically solve L and E_{QQq} .

Except the symmetric case, the light quark can be in a position far from the r-axis. The non-symmetric configuration has been discussed in Ref.[33]. which, as noted in Ref.[33], this string configuration is not energetically favorable. In this paper, we mainly focus on the symmetric configuration.

3 Numerical results and discussion

The system will change from the confined to deconfined phase with increasing temperature. The procedure for determining the melting temperature of QQq is similar to that of QQ \bar{q} . We can judge the melting temperature from the behavior of the potential energy. In the confined phase, if we do not consider string breaking, the potential will rise linearly forever. When changing from a low to high temperature, the behavior of the potential will have an endpoint as shown in the Fig.16. Besides the potential, we can also judge the melting temperature from the behavior of the separation distance. Further discussions can be found in [6, 8, 16, 19].

In this section, we investigate the effect of different temperatures on the QQq potential. The configurations of QQq change with temperature. With an increase in temperature, QQq melts. Because we want to approach the lattice at vanishing temperature, all the parameters are fixed as follows: $s = 0.42 GeV^2$, $\mathbf{g} = 0.176$, $n = 3.057$, $k = -\frac{1}{4}e^{\frac{1}{4}}$, and $c = 0.623 GeV$ [33].

3.1 $T = 0.1 GeV$

First, we investigate the configurations of QQq at the low temperature $T = 0.1 GeV$. At this temperature, the system is in the confined phase with a soft wall below the black-hole horizon and the string and light quark can not exceed this wall[6, 8, 16, 19].

3.1.1 small L

From (17), we can determine the position of the light quark at fixed temperature. The force balance equation of the light quark $F_l(r_q)$ as a function of r_q is presented in Fig. 4(a). where two solutions are observed. However, one solution beyond the soft wall is unphysical. At temperature $T = 0.1 GeV$, $r_q = 1.15 GeV^{-1}$ is a solution of the force balance equation. Then, α can be numerically solved from Eq. (19). The force balance equation for the vertex can give the relationship between the angle α and r_v as shown in Fig. 4(b). In the range $0 \leq r_v \leq r_q$, we find that α is not a monotone function of r_v ; it first decreases and then increases with an increase in r_v . A schematic diagram is shown in Fig. 5.

Furthermore, the separation distance of a heavy-quark pair which can be calculated using Eq. (11) is

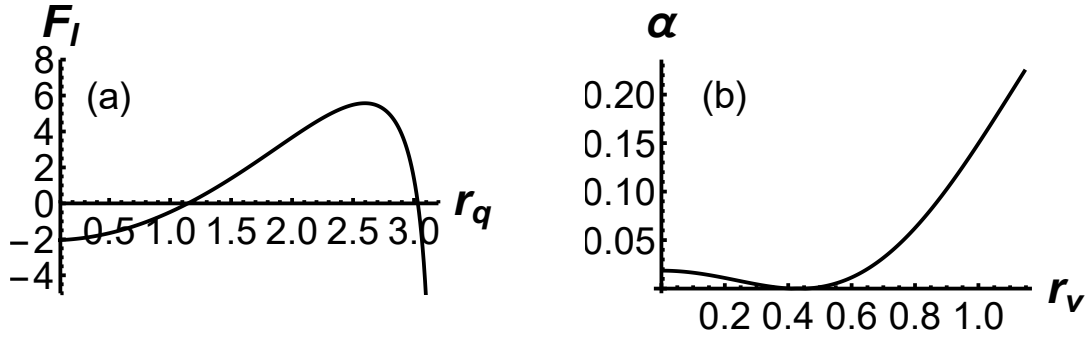


Fig. 4. (a) Force balance equation of the light quark as a function of r_q . (b) α as a function of r_v . The unit for r_q and r_v is GeV^{-1} .

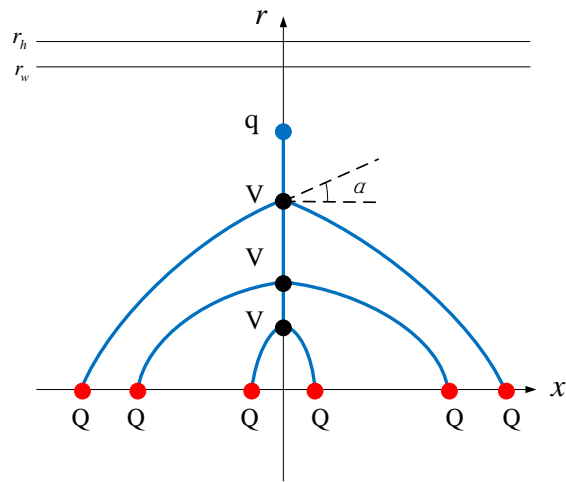


Fig. 5. Schematic diagram of the string configuration with increasing of r_v for small L . α is always positive.

shown in Fig. 6 (a). L is a monotonously increasing function of r_v . At $r_v = r_q$, there is a cutoff. Beyond r_q , the configuration will turn into the second case. The corresponding energy can be calculated using Eq. (15), which is shown in Fig. 6 (b). It is found that the energy is a Coulomb potential at small separation distances and a linear potential at large distances.

3.1.2 Intermediate L

In the second configuration, r_v ranges from r_q to a certain position where α vanishes, as shown in Fig. 7. A schematic diagram for this case is shown in Fig. 8. At the beginning, $\alpha \approx 0.22$. When we increase r_v , α slowly tends to zero.

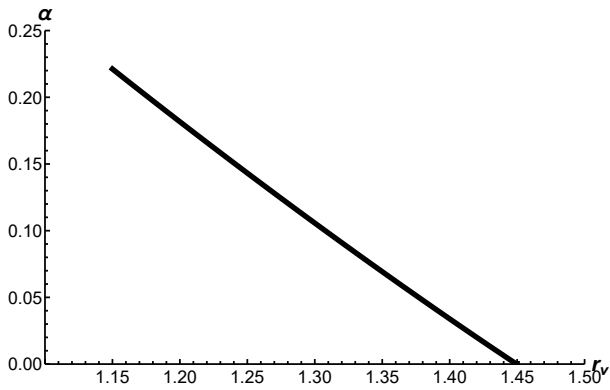


Fig. 7. α as a function of r_v . The unit of r_v is GeV^{-1} .

The separation distance of a heavy-quark pair can also be calculated from Eq. (11). In Fig. 9 (a), we can see that L increases with an increase in r_v . There is an endpoint $r_v = 1.45\text{GeV}^{-1}$, where α tends to zero. Similarly by solving the force balance equation of (24), we obtain numerical results for α . It is found that α is a monotone function of r_v and decreases with an increase in r_v . From Fig. 9 (a), it is clear that the separate distance will increase with increasing r_v . It should be noted that r_v has a maximum value beyond which the configuration will turn to the third case. The maximum separate distance and energy emerge at $r_v = 1.45\text{GeV}^{-1}$. The corresponding energy can also be evaluated, which is shown in Fig. 9 (b). In this configuration, the energy is a linear function of L . Next, we turn to the third case and discuss it further.

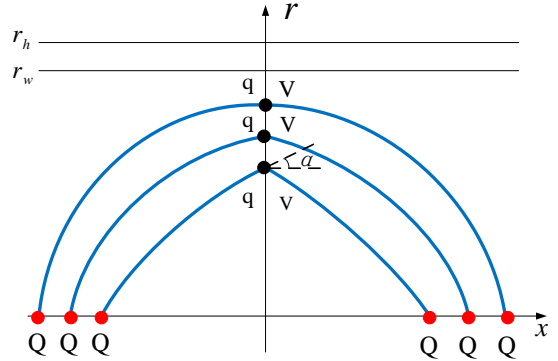


Fig. 8. Schematic diagram of the string configuration with increasing r_v for intermediate L . α is always positive.

3.1.3 large L

Using Eq. (24), we first numerically obtain the relationship between α and r_v , as shown in Fig. 10 (a). Unlike the previous case, the difference here is a negative α . Calculating the first integral from Eq. (29), we find that r_0 is a function of r_v in Fig. 10 (b). As shown, the maximum r_v is $r_v \approx 1.48\text{GeV}^{-1}$, which corresponds to the position of the soft wall $r_w \approx r_0 \approx 1.53\text{GeV}^{-1}$. We can also see that the separation distance tends to infinity when r_0 approaches 1.53GeV^{-1} in Fig. 11 (a).

Finally, the corresponding potential energy is shown in Fig. 11 (b). Because the absolute value of α decreases with increasing r_v , we present a schematic diagram of third configuration in Fig. 12. At $r_0 \approx r_w$, α tends to zero, and the separation distance becomes extremely large.

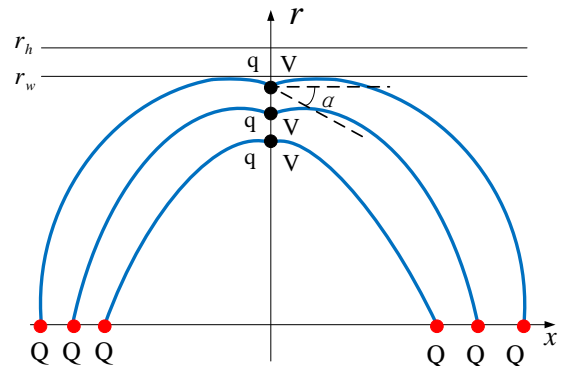


Fig. 12. A schematic diagram of the string configuration with the increase of r_v for large L . α is always negative.

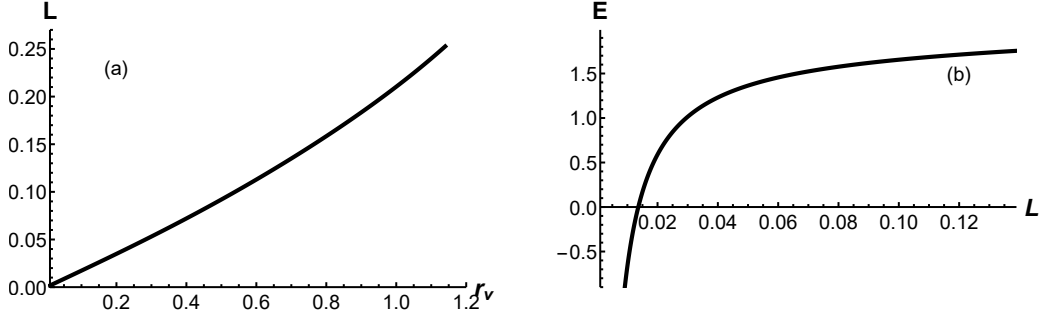


Fig. 6. (a) Separation distance L as a function of r_v . (b) Energy E as a function of separation distance L . The unit of E is GeV, the unit of L is fm and that of r_v is GeV^{-1} .

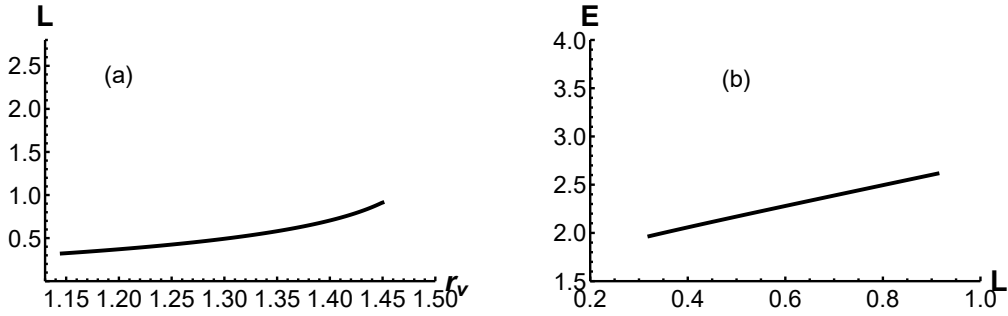


Fig. 9. (a) Separation distance L as a function of r_v . (b) The energy E as a function of L . The unit of E is GeV, the unit of L is fm and that of r_v is GeV^{-1} .

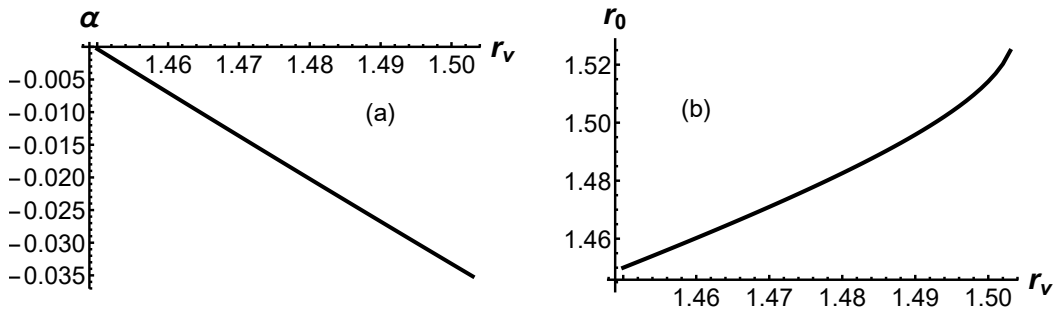


Fig. 10. (a) α as a function of r_v . (b) r_0 as a function of r_v . r_0 and r_v have the unit of GeV^{-1} .

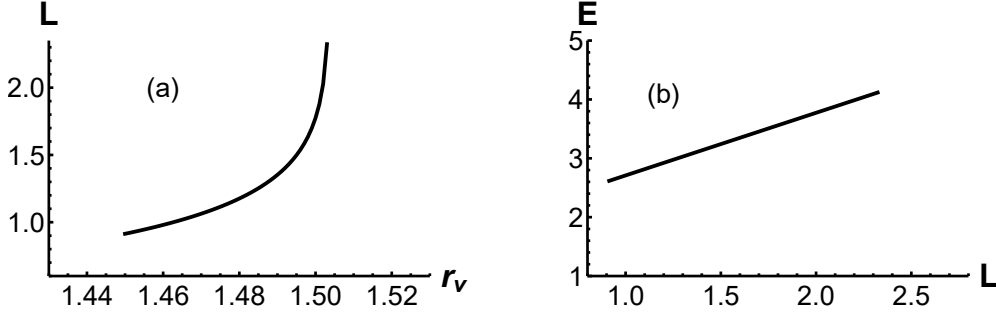


Fig. 11. (a) Separation distance L as a function of r_v . (b) The energy E as a function of L . The unit of E is GeV, the unit of L is fm and that of r_v is GeV^{-1} .

3.1.4 Short summary

If we combine all the configurations, we can present the energy as a function of L at all distances, as shown in Fig. 13. Clearly, the energy is smoothly increasing with separation distance for all configurations.

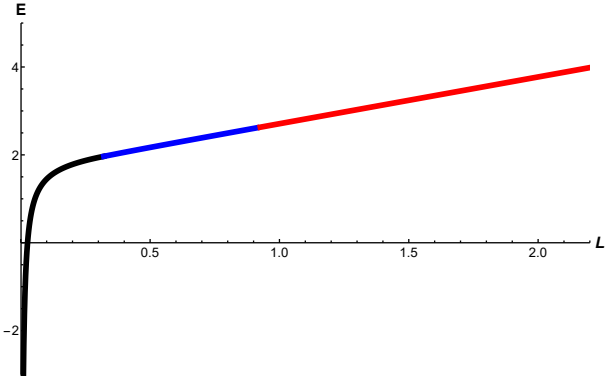


Fig. 13. Energy E as a function of L at all separation distances. The black line represents small distances, the blue line represents intermediate distances, and the red line represents large distances. The unit of E is GeV, and the unit of L is fm.

3.2 $T = 0.148\text{GeV}$

At temperature $T = 0.148\text{GeV}$, the system is in the deconfined phase. In this phase, the soft wall disappears, and the QQq will melt at a sufficient distance.

3.2.1 small L

First, we can determine the position of the light quark from (17). At $T = 0.148\text{GeV}$, we find $r_q = 1.38\text{GeV}^{-1}$ or $r_q = 1.54\text{GeV}^{-1}$. In this paper, we focus on the ground state and only consider $r_q = 1.38\text{GeV}^{-1}$ at $T = 0.148\text{GeV}$. The angle α can be calculated from Eq. (19). The energy and separation distance are calculated using the same procedure as before, and the results are shown in Fig. 14. L is still an increasing function of r_v , and E is a Cornell-like potential.

3.2.2 Intermediate L

In this configuration, we calculate the energy and separation distance in Fig. 15. With an increasing in r_v , the separation distance increases. There is a maximum value $L_{max} = 0.445\text{fm}$ beyond which the configuration can not exist and quarks become free. Thus, we find that the third configuration can't exist at $T = 0.145\text{GeV}$.

3.2.3 Short summary

Only the first and second configurations can exist at $T = 0.148\text{GeV}$. We present the energy as a function of separation distance from 0 to L_{max} in Fig. 16. The potential is smoothly increasing from small distances to intermediate distances. The potential ends at $L_{max} = 0.445\text{fm}$, marked by the red dot in the figure. At large distances, QQq melts and becomes free quarks.

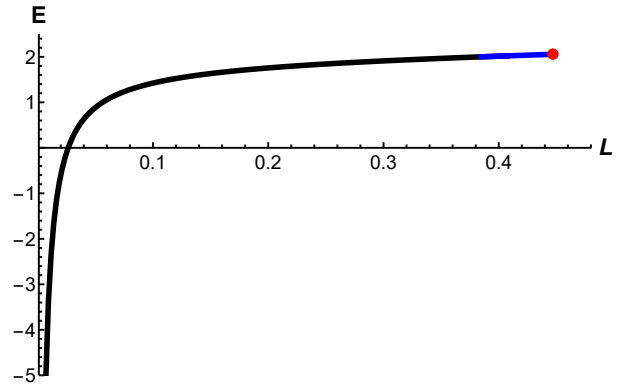


Fig. 16. Energy E as a function of L at all distances. The black line represents E_{QQq} at small distances, the blue line represents E_{QQq} at intermediate distances, and the red line represents E_{QQq} at large distances. The unit of E is GeV, and the unit of L is fm.

3.3 $T = 0.15\text{GeV}$

First, we check the force balance equation of the light quark for the first configuration and find there is no solution for any r_q at $T = 0.15\text{GeV}$, as shown in Fig. 17.

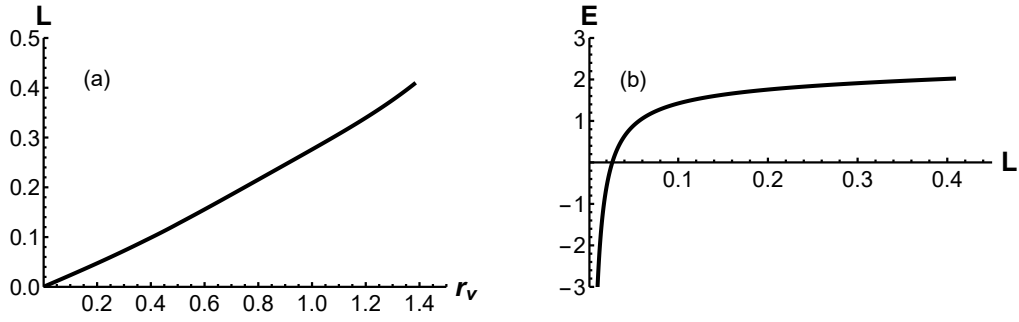


Fig. 14. (a)Separate distance L as a function of r_v . (b)The energy E as a function of L . The unit of E is GeV, L is fm and r_v is GeV^{-1} .

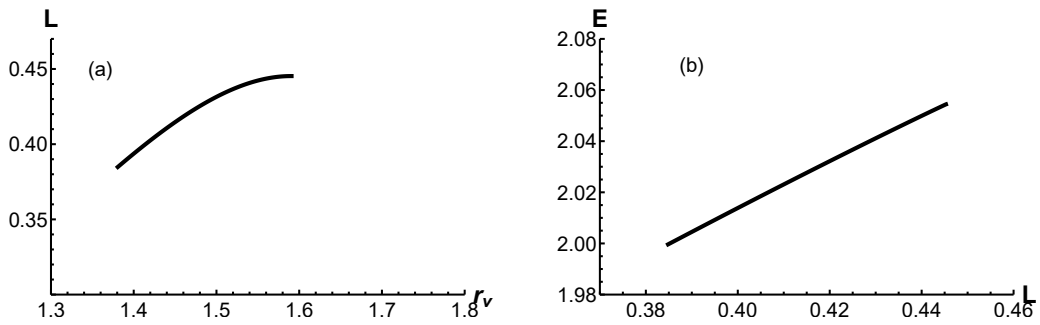


Fig. 15. (a)Separation distance L as a function of r_v . (b)The energy E as a function of L . The unit of E is GeV, the unit of L is fm and that of r_v is GeV^{-1} .

Thus, the first configuration can not exist at this temperature. From Eq. (24), we can find the relationship between α and r_v . There is also a maximum value r_{max} at $T = 0.15 GeV$, beyond which QQq melts as shown in Fig. 18. The separation distance and energy of the string are shown in Fig. 19.

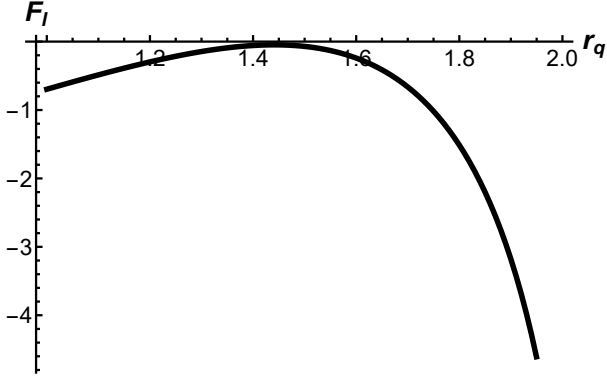


Fig. 17. Force balance equation of the light quark as a function of r_q . The unit of r_q is GeV^{-1}

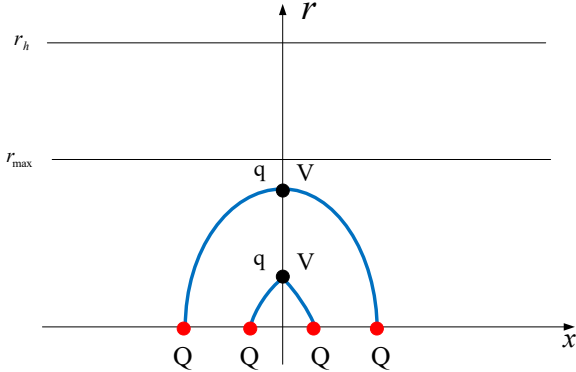


Fig. 18. Schematic diagram of the string configuration with increasing r_v .

4 String breaking in the confined phase

In the confined phase, the quarks are confined in the hadrons. Can QQq exist at extremely large distances? The answer is no. The light quarks and anti-quark will be excited from vacuum at large distances. We call this string breaking and consider the following decay mode

$$QQq \rightarrow Qqq + Q\bar{q}. \quad (35)$$

Qqq consists of three fundamental strings: a vertex and two light quarks. Thus, the total action of Qqq is $S = \sum_{i=1}^3 S_{NG}^{(i)} + S_{vert} + 2S_q$. $Q\bar{q}$ consists of a fundamental string and a light quark. Thus, the total action of $Q\bar{q}$

is $S = S_{NG} + S_q$. The total actions of Qqq and $Q\bar{q}$ are

$$\begin{aligned} S_{Qqq} &= \mathbf{g} \left(2 \int_{r_v}^{r_q} \frac{e^{sr^2}}{r^2} dr + \int_0^{r_v} \frac{e^{sr^2}}{r^2} + 3k \frac{e^{-2sr_v^2} \sqrt{f(r_v)}}{r_v} \right. \\ &\quad \left. + 2n \frac{e^{\frac{1}{2}sr_q^2}}{r_q} \sqrt{f(r_q)} \right), \\ S_{Q\bar{q}} &= \mathbf{g} \int_0^{r_q} \frac{e^{sr^2}}{r^2} + n\mathbf{g} \frac{e^{\frac{1}{2}sr_q^2}}{r_q} \sqrt{f(r_q)}. \end{aligned} \quad (36)$$

Varying the action with respect to r_q gives Eq. (17), and varying the action with respect to r_v gives

$$\begin{aligned} 1 + 3ke^{-3sr_v^3} \sqrt{f(r_v)} + 12kse^{-3sr_v^3} r_v^2 \sqrt{f(r_v)} \\ - \frac{3ke^{-3sr_v^2} r_v f'(r_v)}{2\sqrt{f(r_v)}} = 0. \end{aligned} \quad (37)$$

We can obtain $r_v = 0.410 GeV^{-1}$ or $r_v = 0.453 GeV^{-1}$. Because the difference in energy is extremely small for the two states, we take $r_v = 0.410 GeV^{-1}$ for simplicity. The configuration for $Qqq + Q\bar{q}$ is shown in Fig. 20. The renormalized total energy is

$$\begin{aligned} E_{Qqq} + E_{Q\bar{q}} &= \mathbf{g} \left(2 \int_{r_v}^{r_q} \frac{e^{sr^2}}{r^2} dr + \int_0^{r_q} \left(\frac{e^{sr^2}}{r^2} - \frac{1}{r^2} \right) - \frac{1}{r_q} + \right. \\ &\quad \left. \int_0^{r_v} \left(\frac{e^{sr^2}}{r^2} - \frac{1}{r^2} \right) - \frac{1}{r_v} + 3k \frac{e^{-2sr_v^2} \sqrt{f(r_v)}}{r_v} \right. \\ &\quad \left. + 3n \frac{e^{\frac{1}{2}sr_q^2}}{r_q} \sqrt{f(r_q)} \right) + 2c. \end{aligned} \quad (38)$$

For fixed $r_q = 1.146 GeV^{-1}$ and $r_v = 0.410 GeV^{-1}$, we have $E_{Qqq} + E_{Q\bar{q}} = 3.006 GeV$. Fig.21 is a schematic diagram of string breaking. To determine the string breaking distance, we plot the energy E_{Qqq} and $E_{Q\bar{q}} + E_{Qqq}$ as a function of r_v at $T = 0.1 GeV$ in Fig. 22. The cross point shown in the figure enables us to determine L_{Qqq} at fixed temperature. We find the distance of string breaking to be $L_{Qqq} = 1.27 fm$.

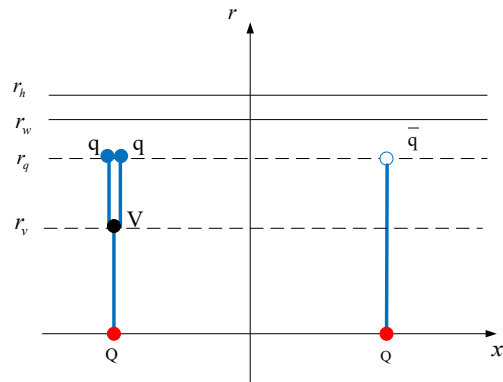


Fig. 20. A schematic diagram of $Qqq + Q\bar{q}$.

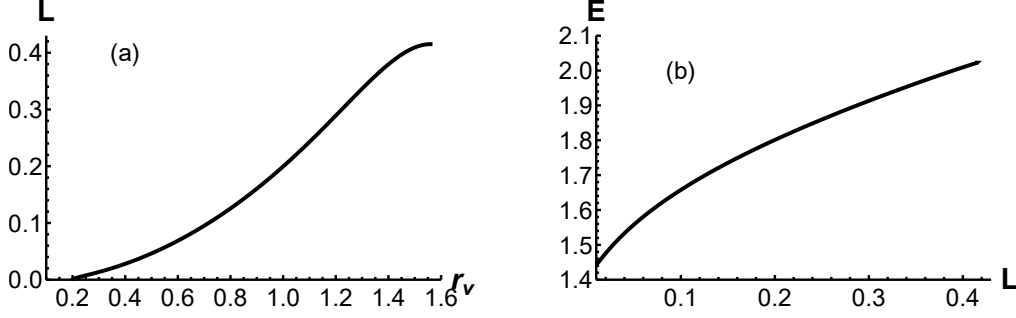


Fig. 19. (a) Separation distance L as a function of r_v . (b) The energy E as a function of L . The unit of E is GeV, the unit of L is fm and that of r_v is GeV^{-1} .

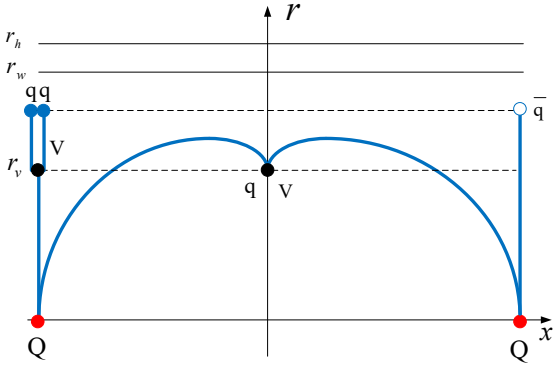


Fig. 21. Schematic diagram of string breaking from the third configuration of QQq to $Qq\bar{q} + Q\bar{q}$.

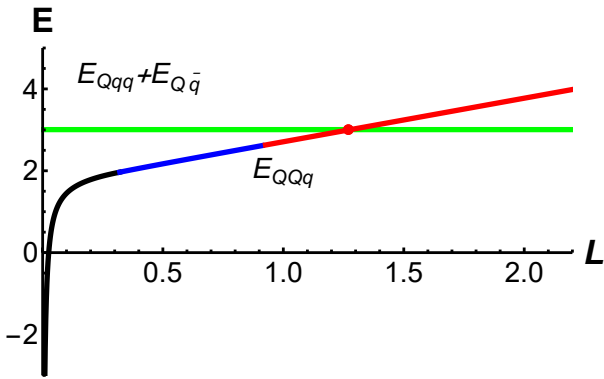


Fig. 22. Green line is the energy $E_{Qq\bar{q}} + E_{Q\bar{q}}$. The black line represents E_{QQq} at small distances, the blue line represents E_{QQq} at intermediate distances, and the red line represents E_{QQq} at large distances. The unit of E is GeV and the unit of r_v is GeV^{-1} .

5 COMPARING WITH $Q\bar{Q}$

The energy of $Q\bar{Q}$ has been extensively studied in many holographic models. In this section, we focus on

comparing the energy of $Q\bar{Q}$ with QQq in the confined and deconfined phases. First, we only show the results of the separation distance and energy of $Q\bar{Q}$

$$L_{Q\bar{Q}} = 2 \int_0^{r_0} \left(\frac{g_2(r)}{g_1(r)} \left(\frac{g_2(r)}{g_2(r_0)} - 1 \right) \right)^{-\frac{1}{2}}, \quad (39)$$

$$E_{Q\bar{Q}} = 2\mathbf{g} \left(\int_0^{z_0} \sqrt{\frac{g_2(r)g_1(r)}{g_2(r) - g_2(r_0)} - \frac{1}{r^2}} - \frac{2\mathbf{g}}{r_0} + 2c \right), \quad (40)$$

where $g_1(r) = \frac{e^{2sr^2}}{r^4}$, $g_2(r) = \frac{e^{2sr^2}}{r^4} f(r)$, and z_0 is the turning point of the U-shape string. A detailed calculation can be found in our previous paper [19, 24, 25]. We consider the decay mode $Q\bar{Q} \rightarrow Q\bar{q} + Qq$. It is clear that

$$E_{Q\bar{q}} = \mathbf{g} \left(\int_0^{r_q} \frac{1}{r^2} (e^{sr^2} - 1) \right) - \frac{\mathbf{g}}{r_q} + \mathbf{g} n \frac{e^{\frac{s}{2} r_q^2}}{r_q} \sqrt{f(r_q)} + c. \quad (41)$$

Thus, we can calculate $E_{Q\bar{q}} + E_{Qq} = 2.39 \text{ GeV}$ at $T = 0.1 \text{ GeV}$. In the confined phase, such as when $T = 0.1 \text{ GeV}$, we present the energy of $E_{Q\bar{q}} + E_{Qq}$ and $E_{Q\bar{Q}}$ in Fig. 23. Trough a comparison with Fig. 22, we find the distance of string breaking $L = 1.25 \text{ fm}$ is close to that of QQq .

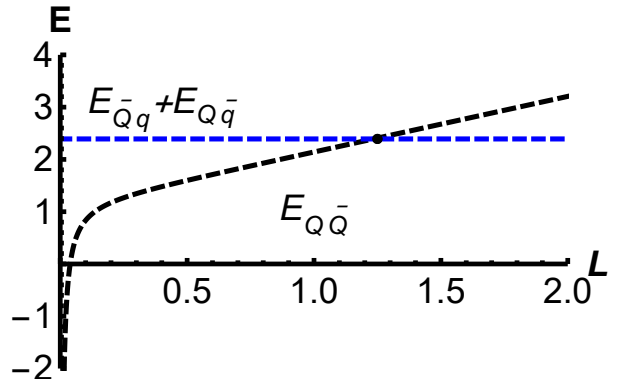


Fig. 23. Blue dashed line is the energy of $E_{Q\bar{q}} + E_{Qq}$, and the black dashed line is the energy of $E_{Q\bar{Q}}$.

$E_{Q\bar{Q}}$. The temperature is $T = 0.1\text{GeV}$. The unit of E is GeV, and the unit of L is fm.

In the deconfinement phase, we compare the energies of $E_{Q\bar{Q}}$ and E_{QQq} at $T = 0.148\text{GeV}$. Fig. 24 shows that the screening distance of $E_{QQq}(L = 0.45\text{fm})$ is significantly smaller than that of $E_{Q\bar{Q}}(L = 0.94\text{fm})$ at the same temperature $T = 0.148\text{GeV}$. This indicates that $Q\bar{Q}$ is more stable than QQq in the deconfined phase.

6 SUMMARY AND CONCLUSION

In this paper, we mainly focused on QQq melting and string breaking at finite temperature through a five-dimensional effective string model. For the confined phase, string and light quarks can not exceed the soft wall. Quarks are permanently confined in the hadrons. However, string breaking of QQq occurs at sufficiently large distances. We considered the decay mode $QQq \rightarrow QQq + Q\bar{q}$ and found the distance of string breaking to be $L = 1.27\text{fm}$. Other decay modes may be considered in the future studies. At a high temperature, the system is in the deconfined phase which implies

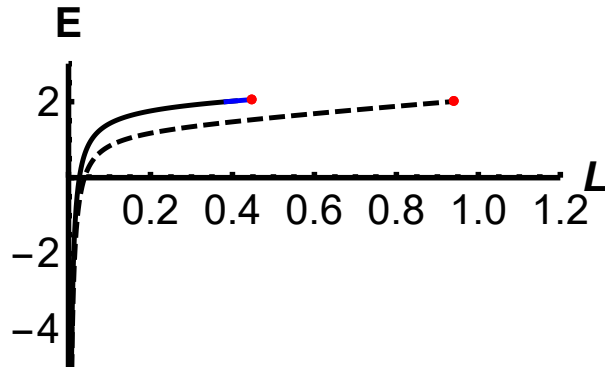


Fig. 24. Solid line is the energy of E_{QQq} , and the dashed line is the energy of $E_{Q\bar{Q}}$. The temperature is $T = 0.148\text{GeV}$. The unit of E is GeV, and the unit of L is fm.

that the soft wall disappears and QQq melts at a certain distance. For example, QQq melts at $L = 0.45\text{fm}$ for $T = 0.148\text{GeV}$. In contrast, we found that $Q\bar{Q}$ melts at $L = 0.94\text{fm}$ for $T = 0.148\text{GeV}$, which indicates that $Q\bar{Q}$ is more stable than QQq at high temperatures. Finally, we hope that studying effective string model will provide more observable quantities for future experiments.

7 Acknowledgments

This work is supported by the NSFC under Grants No. 12175100, No. 11975132 and the Research Foundation of Education Bureau of Hunan Province, China (Grant No. 21B0402, No. 21A0280 and No. 20C1594).

References

- 1 J. M. Maldacena, Phys. Rev. Lett. **80**, 4859-4862 (1998) doi:10.1103/PhysRevLett.80.4859 [arXiv:hep-th/9803002 [hep-th]].
- 2 S. J. Rey, S. Theisen and J. T. Yee, Nucl. Phys. B **527**, 171-186 (1998) doi:10.1016/S0550-3213(98)00471-4 [arXiv:hep-th/9803135 [hep-th]].
- 3 A. Brandhuber, N. Itzhaki, J. Sonnenschein and S. Yankielowicz, Phys. Lett. B **434**, 36-40 (1998) doi:10.1016/S0370-2693(98)00730-8 [arXiv:hep-th/9803137 [hep-th]].
- 4 O. Andreev and V. I. Zakharov, Phys. Rev. D **74**, 025023 (2006) doi:10.1103/PhysRevD.74.025023 [arXiv:hep-ph/0604204 [hep-ph]].
- 5 O. Andreev and V. I. Zakharov, Phys. Lett. B **645**, 437-441 (2007) doi:10.1016/j.physletb.2007.01.002 [arXiv:hep-ph/0607026 [hep-ph]].
- 6 O. Andreev and V. I. Zakharov, JHEP **04**, 100 (2007) doi:10.1088/1126-6708/2007/04/100 [arXiv:hep-ph/0611304 [hep-ph]].
- 7 S. He, M. Huang and Q. s. Yan, Prog. Theor. Phys. Suppl. **186**, 504-509 (2010) doi:10.1143/PTPS.186.504 [arXiv:1007.0088 [hep-ph]].
- 8 P. Colangelo, F. Giannuzzi and S. Nicotri, Phys. Rev. D **83**, 035015 (2011) doi:10.1103/PhysRevD.83.035015 [arXiv:1008.3116 [hep-ph]].
- 9 O. DeWolfe, S. S. Gubser and C. Rosen, Phys. Rev. D **83**, 086005 (2011) doi:10.1103/PhysRevD.83.086005 [arXiv:1012.1864 [hep-th]].
- 10 D. Li, S. He, M. Huang and Q. S. Yan, JHEP **09**, 041 (2011) doi:10.1007/JHEP09(2011)041 [arXiv:1103.5389 [hep-th]].
- 11 K. B. Fadafan, Eur. Phys. J. C **71**, 1799 (2011) doi:10.1140/epjc/s10052-011-1799-7 [arXiv:1102.2289 [hep-th]].
- 12 K. B. Fadafan and E. Azimfard, Nucl. Phys. B **863**, 347-360 (2012) doi:10.1016/j.nuclphysb.2012.05.022 [arXiv:1203.3942 [hep-th]].
- 13 R. G. Cai, S. He and D. Li, JHEP **03**, 033 (2012) doi:10.1007/JHEP03(2012)033 [arXiv:1201.0820 [hep-th]].
- 14 D. Li, M. Huang and Q. S. Yan, Eur. Phys. J. C **73**, 2615 (2013) doi:10.1140/epjc/s10052-013-2615-3 [arXiv:1206.2824 [hep-th]].
- 15 Z. Fang, S. He and D. Li, Nucl. Phys. B **907**, 187-207

- (2016) doi:10.1016/j.nuclphysb.2016.04.003 [arXiv:1512.04062 [hep-ph]].
- 16 Y. Yang and P. H. Yuan, JHEP **12**, 161 (2015) doi:10.1007/JHEP12(2015)161 [arXiv:1506.05930 [hep-th]].
 - 17 Z. q. Zhang, D. f. Hou and G. Chen, Nucl. Phys. A **960**, 1-10 (2017) doi:10.1016/j.nuclphysa.2017.01.007 [arXiv:1507.07263 [hep-ph]].
 - 18 C. Ewerz, O. Kaczmarek and A. Samberg, JHEP **03**, 088 (2018) doi:10.1007/JHEP03(2018)088 [arXiv:1605.07181 [hep-th]].
 - 19 X. Chen, S. Q. Feng, Y. F. Shi and Y. Zhong, Phys. Rev. D **97**, no.6, 066015 (2018) doi:10.1103/PhysRevD.97.066015 [arXiv:1710.00465 [hep-ph]].
 - 20 I. Aref'eva and K. Rannu, JHEP **05**, 206 (2018) doi:10.1007/JHEP05(2018)206 [arXiv:1802.05652 [hep-th]].
 - 21 X. Chen, D. Li and M. Huang, Chin. Phys. C **43**, no.2, 023105 (2019) doi:10.1088/1674-1137/43/2/023105 [arXiv:1810.02136 [hep-ph]].
 - 22 H. Bohra, D. Dudal, A. Hajilou and S. Mahapatra, Phys. Lett. B **801**, 135184 (2020) doi:10.1016/j.physletb.2019.135184 [arXiv:1907.01852 [hep-th]].
 - 23 X. Chen, D. Li, D. Hou and M. Huang, JHEP **03**, 073 (2020) doi:10.1007/JHEP03(2020)073 [arXiv:1908.02000 [hep-ph]].
 - 24 J. Zhou, X. Chen, Y. Q. Zhao and J. Ping, Phys. Rev. D **102**, no.8, 086020 (2020) doi:10.1103/PhysRevD.102.086020 [arXiv:2006.09062 [hep-ph]].
 - 25 J. Zhou, X. Chen, Y. Q. Zhao and J. Ping, Phys. Rev. D **102**, no.12, 126029 (2021) doi:10.1103/PhysRevD.102.126029
 - 26 X. Chen, L. Zhang, D. Li, D. Hou and M. Huang, [arXiv:2010.14478 [hep-ph]].
 - 27 X. Chen, L. Zhang and D. Hou, [arXiv:2108.03840 [hep-ph]].
 - 28 R. Aaij *et al.* [LHCb], Phys. Rev. Lett. **119**, no.11, 112001 (2017) doi:10.1103/PhysRevLett.119.112001 [arXiv:1707.01621 [hep-ex]].
 - 29 R. Aaij *et al.* [LHCb], Phys. Rev. Lett. **121**, no.16, 162002 (2018) doi:10.1103/PhysRevLett.121.162002 [arXiv:1807.01919 [hep-ex]].
 - 30 Y. L. Ma and M. Harada, J. Phys. G **45**, no.7, 075006 (2018) doi:10.1088/1361-6471/aac86e [arXiv:1709.09746 [hep-ph]].
 - 31 A. Yamamoto, H. Suganuma and H. Iida, Phys. Rev. D **78**, 014513 (2008) doi:10.1103/PhysRevD.78.014513 [arXiv:0806.3554 [hep-lat]].
 - 32 J. Najjar and G. Bali, PoS **LAT2009**, 089 (2009) doi:10.22323/1.091.0089 [arXiv:0910.2824 [hep-lat]].
 - 33 O. Andreev, JHEP **05**, 173 (2021) doi:10.1007/JHEP05(2021)173 [arXiv:2007.15466 [hep-ph]].
 - 34 O. Andreev, Phys. Lett. B **756**, 6-9 (2016) doi:10.1016/j.physletb.2016.02.070 [arXiv:1505.01067 [hep-ph]].
 - 35 O. Andreev, Phys. Rev. D **93**, no.10, 105014 (2016) doi:10.1103/PhysRevD.93.105014 [arXiv:1511.03484 [hep-ph]].
 - 36 O. Andreev, Phys. Lett. B **804**, 135406 (2020) doi:10.1016/j.physletb.2020.135406 [arXiv:1909.12771 [hep-ph]].
 - 37 O. Andreev, Phys. Rev. D **104**, no.2, 026005 (2021) doi:10.1103/PhysRevD.104.026005 [arXiv:2101.03858 [hep-ph]].
 - 38 A. Yamamoto, H. Suganuma and H. Iida, "Heavy-heavy-light quark potential in two approaches," Prog. Theor. Phys. Suppl. **174**, 270-273 (2008).
 - 39 A. Karch, E. Katz, D. T. Son and M. A. Stephanov, Phys. Rev. D **74**, 015005 (2006) doi:10.1103/PhysRevD.74.015005 [arXiv:hep-ph/0602229 [hep-ph]].
 - 40 O. Andreev, Phys. Rev. D **73**, 107901 (2006) doi:10.1103/PhysRevD.73.107901 [arXiv:hep-th/0603170 [hep-th]].
 - 41 O. Andreev, Phys. Rev. D **76**, 087702 (2007) doi:10.1103/PhysRevD.76.087702 [arXiv:0706.3120 [hep-ph]].
 - 42 E. Witten, JHEP **07**, 006 (1998) doi:10.1088/1126-6708/1998/07/006 [arXiv:hep-th/9805112 [hep-th]].
 - 43 O. Andreev, Phys. Rev. D **101**, no.10, 106003 (2020) doi:10.1103/PhysRevD.101.106003 [arXiv:2003.09880 [hep-ph]].